Ab-Initio Studies of Large Deformation Processes of Graphene

Peter W. Chung[1]

Summary

Full potential energy surfaces for periodic graphene sheets under large uniaxial deformations have been generated using ab initio and empirical methods. Under the constrained loading conditions, internal rotations of bonds are observed similar to Stone-Wales transformations in the absence of temperature effects. The zero temperature energy landscapes reveal multiple metastable states emanating from the original configuration that suggest a bifurcation phenomenon and multiple energetically equivalent kinetic pathways that result in reduction in the lattice symmetry due purely to mechanical activation. A local trapping effect created by the small primitive cell also leads to a computed activation energy of 1.3 eV, which is significantly lower than previous theoretical results.

Introduction

It is commonly recognized that the Stone-Wales transformation [1] is an important atomistic mechanism in the mechanical deformation of fullerenes and graphitic systems under tension [2]–[10]. The rotation of a single bond changes the local coordination of the carbon atoms where the new configuration is energetically more favorable and relieves the amount of strain energy the system must withstand [3]. Studies to date have emphasized significant importance on this transformation because of its unique consequence to the mechanical behavior of nanotubes, the implications for graphite in-plane diffusion and other related studies notwithstanding [2],[11]–[13]. The dislocation dipole created by the bond rotation "unlocks" the plasticity mechanism and serves as the core from which dislocations can emanate [7] which can then ultimately lead to fracture [8]. In axial nanotube tension and at high temperatures, the formation of the defect has also been shown to be reversible [3] and substantially influenced by the curvature of the nanotube [10]. Long time effects, more representative of laboratory time scales, have also been shown through simulation to be a key consideration in nanotube yield [14].

Whereas early calculations show a nanotube tensile yield strain of $> 30\%$ [15], the (5/7/7/5) defect can successfully be created under smaller strains, typically above 5% at non-zero temperature [3],[6],[16] but smaller than the brittle fracture strain of 12-16% [17]. A Stone-Wales defect activation energy around 6-8 eV

[1]Computational and Information Sciences Directorate, U.S. Army Research Laboratory, AMSRL-CI-HC, Aberdeen Proving Ground, MD 21005-5067, pchung@arl.army.mil, Phone: (410) 278-6027, Fax: (410) 278-4983.

appears to be the recent concensus via both theory [4],[10],[18] and experiment [12] despite lower (3.92 eV by [11]) and higher (10.4 eV [2] and 9.8 eV [13]) estimates. However, these high barrier values have thus far been significantly different from the observed low tensile strength of single (SWNT) and multiwall (MWNT) carbon nanotubes. Experiments consistently show tensile strengths (10-150 GPa [19],[20] lower than numerical and theoretical estimates of 150-400 GPa [15],[19]. Furthermore, the direct exchange mechanism that comprises the SW transformation is typically assumed to be a symmetric rotation around a single bond. Recent work [5] has shown this to be unlikely, particularly in the context of out-of-plane motions of the atoms involved in the rotating bond.

These observations raise the following question: Is there a lower energy pathway for the exchange mechanism to occur in graphene? In this paper, detailed strain energy landscapes are computed using Density Functional Theory with respect to an applied non-dilatational deformation. Two sets of calculations are performed and compared. The first comes from the planewave ABINIT code [21], in which the exchange and correlation term is treated through the generalized gradient approximation (GGA) according to the Perdew-Burke-Ernzerhof functional with the Hartwigsen-Goedecker-Hutter pseudopotential for carbon. A planewave energy cutoff of 1360 eV is used throughout. The second is through the Tersoff-Brenner (TB) bondorder potential [22],[23].

Computational Approach

The calculations proceed by taking the primitive cell of single crystal graphene containing two atoms. One atom is held fixed while the position of the other atom is varied in the plane to perform energy scans over a fixed grid throughout the entire cell. There is no loss of generality in this approach because of the translational symmetry of the Bravais cell. At each deformation state, 2200 grid points are evaluated. Each grid point represents a single SCF calculation and the points combine to generate a full energy landscape. The stable locations are identified by searching through for local positive definite regions over the energy landscape. The key computed variables are the strain energy (E), the activation energy (E_a), and the formation energy (E_f) all with respect to the applied deformation tensor (F_{ij}). Computations were performed on a Linux NetworX Evolocity II cluster containing 256 Intel 3.06 GHz processors running Red Hat Enterprise Linux.

The present computations are limited to in-plane motions of the atoms only. We note however that out-of-plane stable structures have before been predicted to reduce the energy by as much as 0.6 eV [5] over a large range of deformations. Additionally, defect formation has been shown to be strongly influenced by chiral

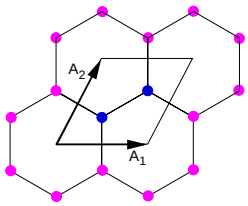

Figure 1: Primitive cell of graphene. Dark atoms denote primitive cell atoms, light atoms are periodic images.

nanotubes, or the direction of applied strain [9]. The formation energy is consistently lowest for the arm-chair configuration [3],[7],[9]. For this reason, the present results report only deformation along the zig-zag axis with the arm-chair direction held fixed.

Two calculations schemes were employed here - DFT-GGA [21] and the TB classical potential [22],[23]. The reference energies and nearest-neighbor distances are for GGA (E_o=-309.969 eV,r_o=1.42489Å) and for the TB potential (E_o=-7.37563 eV,r_o=1.45068Å). The GGA energy contains total contributions from the kinetic, hartree, XC, Ewald, core, local and nonlocal pseudopotential energies.

Results and Discussion

Calculations of E are shown in Figure 2 in the unloaded reference state and at 29% strain. The cell dimensions for all states of strain are scaled to unity. The location of the minima in the undeformed results are nearly identical. For the fixed position of the first atom at the reduced coordinate of (1/3,1/3), the equilibrium position of the second atom is clearly at (2/3,2/3). The additional minima at (1,0), (1,1), and (0,1) are due to the frame invariance of the hexagonal structure of graphene. In the undeformed reference calculations, the largest discrepancy occurs at 2 eV where the TB potential shows a local minimum at approximately the (1/3,5/6) point as well as its frame invariant three-fold symmetric counterparts. Thus, whereas the TB potential predicts an alternate reduced symmetry crystal structure with an activation barrier of approximately 2 eV at zero strain, no such structure can be found in the GGA result.

The landscapes at 29% applied strain are markedly different despite showing the same qualitative local minima. All energy values are taken relative to the corresponding E_o described earlier. Both methods show a reduction of three-fold symmetry – there are now two additional alternate local minima in the cell. Figure 2(b) shows distinct regions at cell locations (1/3,5/6) and (5/6,5/6) at energetically

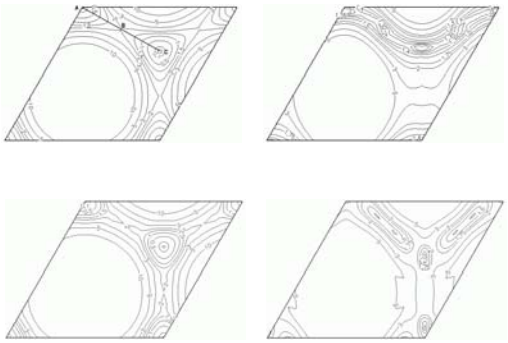

Figure 2: Strain energy landscape over primitive cell. Computations using GGA at (upper left) zero strain and (upper right) 29% strain and Tersoff-Brenner empirical potential using (lower left) zero strain and (lower right) 29% strain.

equivalent levels of 1.32 eV. A kinetic pathway, or direct exchange channel, is created by the deformation that appears to make the bond-rotated configuration energetically feasible and favorable. The barrier to the motion is approximately 0.05 eV at this deformation. Figure 2(d) shows the minima at qualitatively similar locations but in an elongated local well terminated by two smaller sub-minima at an energy level of 1.4 eV. The channel is less well-defined showing a barrier of approximately 0.55 eV. In both sets of calculations, the relative positions of the minima remains nearly constant throughout the deformations, indicating that through these constrained motions the partial bond rotation is metastable and invariant for larger strains. The subsequent crystals of reduced symmetry will be discussed in the final paper.

Figures 2 also show a remarkable difference that may have direct consequence on structure optimization calculations. At the largest energy contour level shown (5 eV), and at lower levels not shown, the contour lines take on a nonsmooth characteristic that is attributable to the cutoff function in the empirical potential. Although these are at a relatively higher energy level compared to the minimum energy, search algorithms may face significant difficulty converging if improperly sized line-search parameters are employed.

The zero temperature deformation at which the bond-rotation becomes energetically favorable is consistent in both GGA and TB at approximately 30% strain. Figure 3 depicts the energy levels along the line ABC in Figure 2(a). We see again, however, the strong discontinuity in energy from TB at larger extents of deforma-

tion where it is arguable whether the cutoff parameters for the potential are still valid. It is once again noteworthy that stable local minima appear in TB that are not present in GGA when no deformation is present.

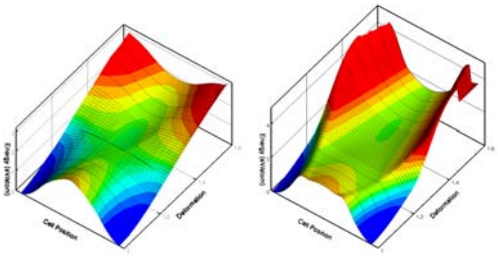

Figure 3: Energy with respect to deformation along line ABC of Figure 2(a) using (left) GGA and the (right) TB potential.

Closing Remarks

The approximation introduced by using the small (primitive cell) computational domain means we are inherently considering a constrained, lattice-trapped system. This suggests that the deformations proposed are unrealistic outside of zero temperature lattice statics. However, at higher temperatures among thermal oscillations such trapped configurations may make the lower energy pathways instantaneously accessible and, in fact, more favorable. These results therefore reveal mechanisms previously unconsidered in the deformation of and diffusion in planar graphene lattices.

Acknowledgements

The author gratefully acknowledge the support from the U.S. Army Research Laboratory Director's Research Initiative Award (DRIFY04). Significant computer resources were made available through the U.S. Army Research Laboratory Major Shared Resource Center.

Reference

1. Stone, A. J.; Wales, D. J. (1986): *Chem. Phys. Lett.*, 128, 501.
2. Kaxiras, E.; Pandey, K. C. (1988): *Phys. Rev. Lett.*, 61, 2693.
3. Nardelli, M. B.; Yakobson, B. I.; Bernholc, J. (1998): *Phys. Rev. B*, 57, 4277.
4. Samsonidze, Ge. G.; Samsonidze, Gu. G.; Yakobson, B. I. (2002): *Phys. Rev. Lett*, 88, 065501.
5. Samsonidze, Ge. G.; Samsonidze, G. G.; Yakobson, B. I. (2002): *Comp. Mater.*

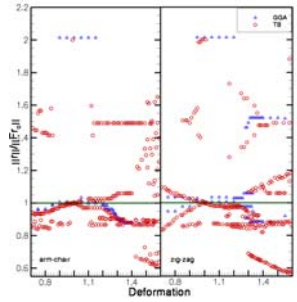

Figure 4: Magnitudes of the stable interatom distance of C-atoms in primitive cell with respect to deformation.

Sci., 23, 62.

6. Troya, D.; Mielke, S. L.; Schatz, G. C. (2003): *Chem. Phys. Lett.*, 382, 133.
7. Yakobson, B. I. (1998): *Appl. Phys. Lett.*, 72, 918.
8. Yakobson, B. I.; Samsonidze, G.; Samsonidze, G. G. (2000): *Carbon*, 38, 1675.
9. Zhang, P.; Lammert, P. E.; Crespi, V. H. (1998): *Phys. Rev. Lett.*, 81, 5346.
10. Zhou, L. G.; Shi, S.-Q. (2003): *Appl. Phys. Lett.*, 83, 1222.
11. Dienes, G. J. (1952): *J. Appl. Phys*, 23, 1194.
12. Kanter, M. A. (1957): *Phys. Rev.*, 107, 655.
13. Xu, C. H.; Fu, C. L.; Pedraza, D. F. (1993): *Phys. Rev. B*, 48, 13273.
14. Wei, C.; Cho, K.; Srivastava, D. (2003): *Phys. Rev. B*, 67, 115407.
15. Yakobson, B. I.; et al. (1997): *Comp. Mater. Sci.*, 8, 341.
16. Walters, D. A.; et al. (1999): *Appl. Phys. Lett.*, 74, 3803.
17. Omeltchenko, A.; Yu, J.; Kalia, R. K.; Vashishta, P. (1997): *Phys. Rev. Lett.*, 78, 2148.
18. Crespi, V. H.; Benedict, L. X.; Cohen, M. L.; Louie, S. G. (1996): *Phys. Rev. B*, 53, 13303.
19. Demczyk, B. G.; et al. (2002): *Mat. Sci. Eng. A*, 334, 173.
20. Yu, M.-F.; et al. (2000): *Science*, 287, 637.
21. Gonze, X.; et al. (2002) *Comp. Mater. Sci.*, 25, 478.
22. Tersoff, J. (1988): *Phys. Rev. Lett.*, 61, 2879.
23. Brenner, D. W. (1990): *Phys. Rev. B*, 42, 9458.